

Accuracy control in ultra-large-scale electronic structure calculation

T. Hoshi^{1,2} ‡

¹ Department of Applied Physics, University of Tokyo, 7-3-1 Hongo, Bunkyo-ku, Tokyo 113-8656, Japan

² Core Research for Evolutional Science and Technology (CREST-JST), Japan Science and Technology Agency, 4-1-8 Honcho, Kawaguchi-shi, Saitama 332-0012, Japan

E-mail: hoshi@damp.tottori-u.ac.jp

Abstract. Numerical aspects are investigated in ultra-large-scale electronic structure calculation. Accuracy control methods in process (molecular-dynamics) calculation are focused. Flexible control methods are proposed so as to control variational freedoms, automatically at each time step, within the framework of generalized Wannier state theory. The method is demonstrated in silicon cleavage simulation with 10^2 - 10^5 atoms. The idea is of general importance among process calculations and is also used in Krylov subspace theory, another large-scale-calculation theory.

‡ Present address: Department of Applied Mathematics and Physics, Tottori University, 4-101 Koyama-Minami, Tottori, 680-8550 Japan

1. Introduction

Nowadays one of most important scientific fields is process of nanostructure, structure in nanometer- or ten-nanometer scales, particularly, for controllability of its structure and function. Electronic structure calculation in these purposes should be carried out with a large system (10^3 atoms or more) and a meaningful timescale. For a decade, on the other hand, many calculation methods and related techniques have been proposed so as to handle such large systems. See reviews [1, 2] and original works. [3, 4, 5, 6, 7, 8, 9, 10, 11, 12, 13, 14, 15, 16, 17, 18, 19, 20, 21, 22] In these methodologies, one-body density matrix or Green's function is calculated, instead of one-electron eigenstates and the calculation is carried out with real-space representation. A physical quantity $\langle X \rangle$ is given as a trace form

$$\langle X \rangle = \text{Tr}[\rho X] = \int \int d\mathbf{r} d\mathbf{r}' \rho(\mathbf{r}, \mathbf{r}') X(\mathbf{r}', \mathbf{r}). \quad (1)$$

with the density matrix ρ . If the matrix $X(\mathbf{r}, \mathbf{r}')$ is of short range, the off-diagonal long-range component of the density matrix does not contribute to the physical quantity $\langle X \rangle$, which is crucial for practical success of large-scale calculations. [7]

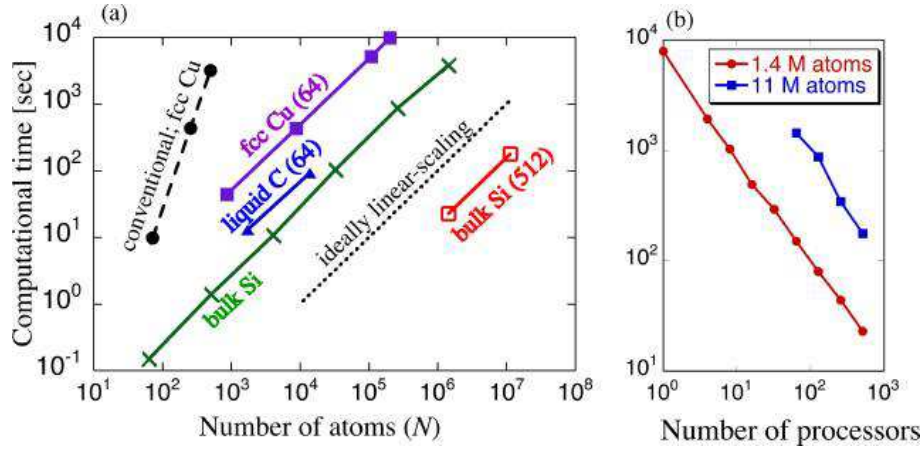


Figure 1. (color online) Computational time of the ultra-large-scale calculation with up to 11,315,021 atoms. The time of our methods are plotted for fcc Cu, liquid C and bulk Si. Optimal solver method is chosen for each system; [21] Wannier state theory in perturbative procedure is chosen for bulk silicon and Krylov subspace theory is chosen for other cases. (a) Comparison among materials. As a reference data, the time of the conventional eigenstate calculation is also plotted for fcc Cu with single CPU. See Refs. [15, 17, 21] for details. The computations were carried out using Intel or SGI CPUs. In parallel computation, the number of processors (CPU cores) is indicated inside the parenthesis. (b) The time of bulk silicon with 1,423,909 atoms and 11,315,021 atoms, is measured as a function of processors using SGI origin 3800TM.

As ones of these works, we have developed a set of theories and program codes and applied them to silicon, carbon and metal systems with Slater-Koster-form Hamiltonians. [15, 16, 17, 19, 20, 21] These theories are constructed from fundamental theory of generalized Wannier state or Krylov subspace. An overview is given in Ref. [21].

Figure 1 demonstrates our methods with or without parallel computers, in which the computational cost is ‘order- N ’ or linearly proportional to the system size (N), up to ten-million atoms and shows a satisfactory performance in parallel computation. We note that the electronic property, such as density of states, is also calculated. [16, 19, 21]

These large-scale-calculation methods have controlling parameters for calculating electronic freedoms, which gives accuracy and computational cost. In the present paper, we will introduce flexible methods of controlling electronic freedoms for optimal computational cost, and will be demonstrated within the framework of generalized Wannier state theory. The methods are crucial, particularly, in a dynamical process or a molecular dynamics (MD) calculation. This paper is organized as follows; An overview of theory and example of silicon cleavage are given in Sec 2. Then the flexible control methods are introduced and demonstrated in Sec. 3. We point out that similar flexible control methods are used in Krylov subspace theory. Section 4 is devoted to concluding remarks.

2. Theoretical overview and examples

The calculation in this paper was carried out in the theoretical framework of generalized Wannier state. [23, 24, 3, 5, 25, 10, 26, 27, 28, 29] A physical picture of the generalized Wannier states $\{\phi_i^{(\text{WS})}\}$ is localized chemical wave function in condensed matters, such as a bonding orbital or a lone-pair orbital with a slight spatial extension or ‘tail’. The suffix i of a wavefunction $\phi_i^{(\text{WS})}$ indicates the position of its localization center, such as bond site. Their wavefunctions $\{\phi_i^{(\text{WS})}\}$ are equivalent to the unitary transformation of occupied eigen states and the density matrix is given as

$$\rho(\mathbf{r}, \mathbf{r}') = \sum_{j=1}^{\text{occ.}} \phi_j^{(\text{WS})}(\mathbf{r}), \phi_j^{(\text{WS})}(\mathbf{r}') \quad (2)$$

where wavefunctions are described as real number. The Wannier state theory is suitable for large systems, particularly, when a dominant number of wavefunctions are well localized. The present calculations were carried out by a variational procedure [10, 21, 29]

Hereafter silicon cleavage process is calculated with a transferable Hamiltonian in the Slater-Koster form [30]. Nanometer-scale or ten-nano-meter-scale samples are cleaved under external load. Figure 2 shows examples of the resultant cleaved samples that contain experimentally observed cleavage planes, (111) and (110) planes; In Fig, 2(a), the resultant sample contains a cleaved Si(111)-2×1 surface. [17] A pair of five- and seven-membered rings appears in the cleavage propagation direction, $[2\bar{1}\bar{1}]$ direction, which forms the unit cell of the 2×1 structure called Pandey structure. [31, 32, 33] As an interesting feature of the present result, the cleaved surface contains a step structure with a six-membered ring at the step edge, which is compared to experiments. [17] As details, the sample consists of 1,112 atoms and the periodic boundary condition is imposed, by eight atomic layers, in the direction perpendicular to the cleavage propagation direction. In the present case, an additional periodicity, by two atomic layers, is imposed as a

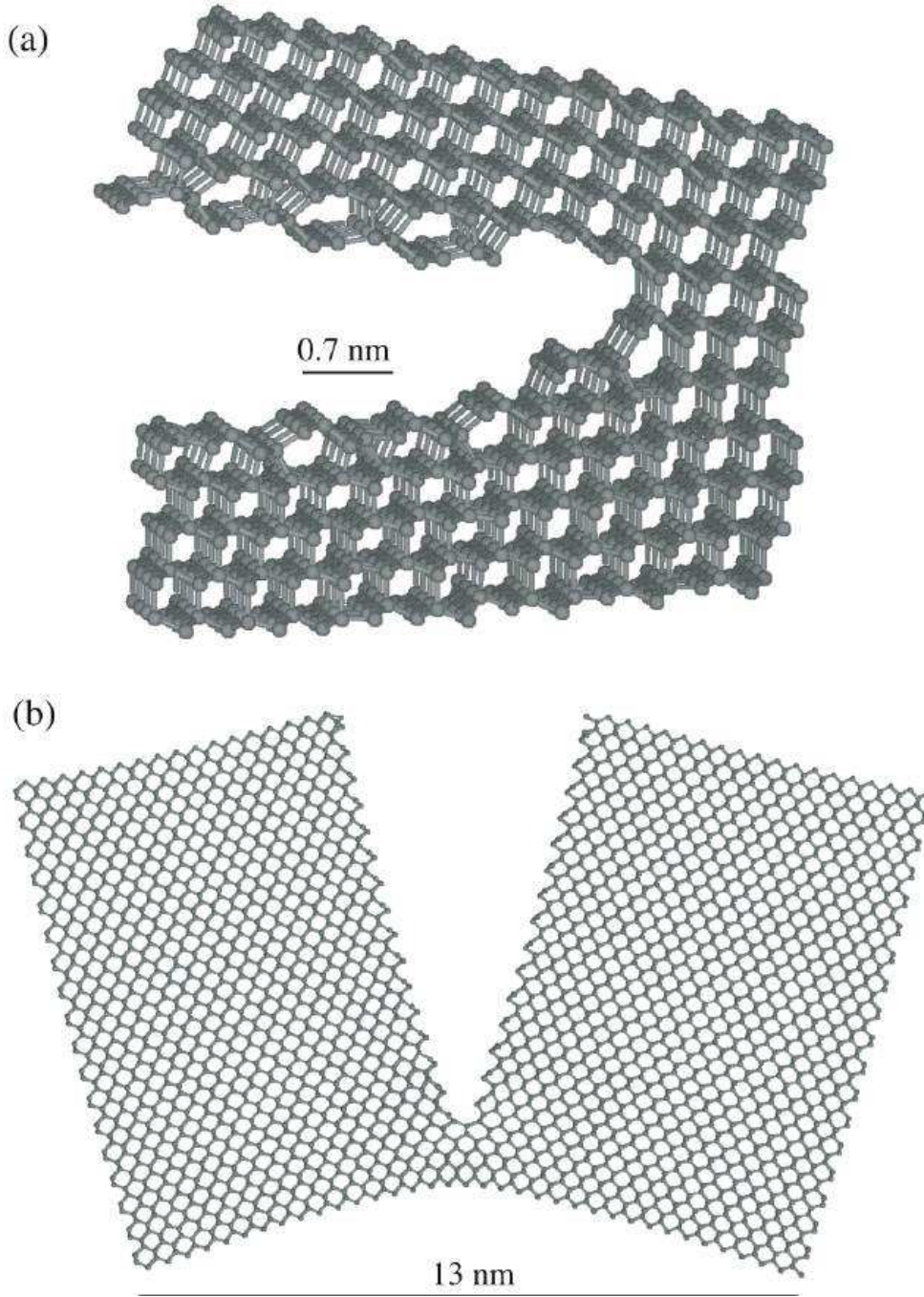


Figure 2. (color online) Simulation results of silicon cleavage. (a) A sample with 1,112 atoms. The resultant cleaved surface shows a (111)-2 \times 1 reconstruction and contains a step structure. (b) A sample with 10,368 atoms. The resultant cleaved surface shows a buckled (110) reconstruction.

constraint on the atomic structure. We note that the 2x1 structure appears even without the additional periodicity. See papers [17] for more details and results of larger samples with 10^5 atoms. In Fig. 2(b), the resultant cleaved surface is a buckled (110) surface that appears in textbooks in surface physics or papers such as Refs. [34, 35]. As details, the

sample consists of 10,368 atoms and the periodic boundary condition is imposed, by eight atomic layers, in the direction perpendicular to the cleavage propagation direction. The physical discussions in cleavage dynamics are found in Refs. [15, 17, 21] and reference therein.

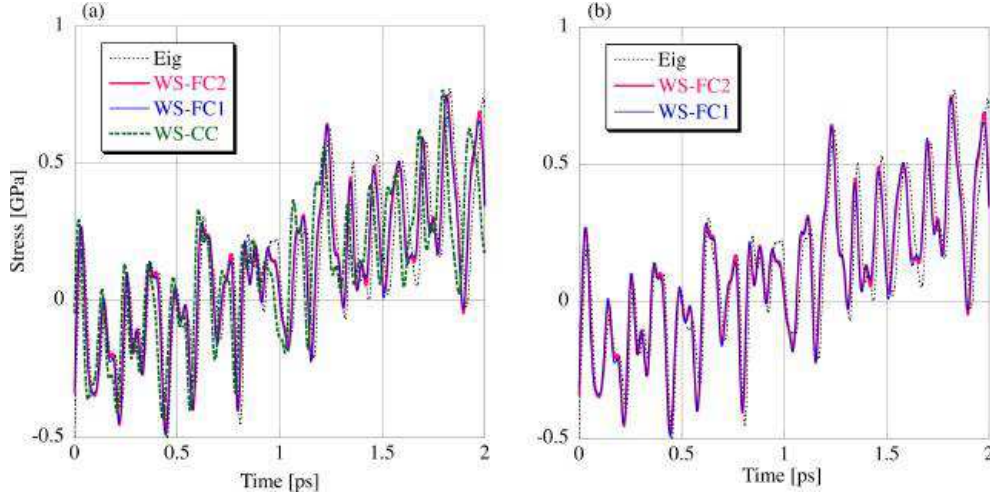


Figure 3. (color online) (a) The stress value of nanocrystalline silicon of 91 atoms with thermal vibration, in which the sample is stretched by a [001] uniaxial load. The calculations were carried out by the Wannier state method with (i) ‘constant cutoff’ (WS-CC), (ii) ‘flexible control at the first level’ (WS-FC1), and (iii) ‘flexible control at the second level’ (WS-FC2). See text for explanation. The conventional eigen state method (Eig) was also carried out as a reference data. (b) The same data set as in (a) are plotted but the data of the CC method is ignored, so as to clarify a significantly better agreement among the other methods.

3. Flexible methods for accuracy control

3.1. Three methods in Wannier state theory

Here we describe the accuracy control methods [15, 17, 29] used in the above MD calculation. In generalized Wannier state theory, the region for localization constraint for each Wannier state is variational freedoms that governs accuracy and computational cost. Therefore we will concentrate the methods of setting the localization region for each wavefunction at each time step.

Here the three methods of accuracy control in the Wannier state calculation are proposed. Among all the methods, the localization constraint on each wavefunction $\phi_i^{(\text{WS})}$ is imposed as a spherical region whose center is the weighted center of the wavefunction $\mathbf{r}_i^{(\text{WS})} \equiv \langle \phi_i^{(\text{WS})} | \hat{\mathbf{r}} | \phi_i^{(\text{WS})} \rangle$. Therefore, the cutoff radius of the spherical region, denoted $R_i^{(\text{WS})}$, mainly contributes to accuracy. We also denote $N_i^{(\text{WS})}$ as the number of atoms inside the localization region of the i -th Wannier state. Three methods for determination of the radius are used; (i) ‘constant cutoff’ method (WS-CC method)

(ii) ‘flexible control method at the first level’ (WS-FC1 method), and (iii) ‘flexible control method at the second level’ (WS-FC2 method). See below for explanation of these methods.

The method is demonstrated in nanocrystalline silicon of an isolated cubic sample with 91 atoms. [29] The sample is thermally vibrated with 300 K and an additional slow constant-velocity motion is introduced for the atoms on the sample surface. As a result, the sample is stretched in the [001] direction with thermal vibration. Figure 3 shows the trajectory of calculated stress σ . In Fig.3(a), the results of three controlling methods for Wannier states are compared. Figure 3(a) also contains a result of conventional eigen-state calculation as a reference data, in which the temperature (level-broadening) parameter of $\tau = 0.1$ eV is used for electronic system.

In the WS-CC method of Fig. 3, the radius is chosen to be a constant value of $R_i^{(\text{WS})} = 2.5d_0$, where $d_0 (= 2.35\text{\AA})$ is the equilibrium bond length. This value is chosen for all Wannier states through the simulation. Without an external load, this radius sets the localization region of the Wannier states to about $N_i^{\text{WS}} = 40$ atoms. We should say that a results with the CC method is expected to be rather poor, because the sample in the present MD simulation will be stretched by the external load and the number of atoms within the localization region tends to decrease during the MD simulation. This point will be confirmed numerically in the last paragraph of the present subsection.

A better way for accuracy control is to give the number of atoms in the localization region, N_i^{WS} , instead of a given radius $R_i^{(\text{WS})}$, which realized a flexible control for the localization radius. In this method, the radius $R_i^{(\text{WS})}$ is chosen so that the localization region contains a given number, $N_i^{(\text{WS},\text{min})}$, of atoms or more. This method is called flexible control method at the first level (WS-FC1 method). In Fig. 3(a) we choose the value of $N_i^{(\text{WS},\text{min})} = 40$. In results, the localization radius $R_i^{(\text{WS})}$ may be different among the Wannier states and the number of atoms within the localization region (N_i^{WS}) always satisfies $N_i^{(\text{WS})} \geq N_i^{(\text{WS},\text{min})} = 40$.

Now we explain the third method for setting the localization region, called flexible control method at the second level (WS-FC2 method). In the program code, an iterative solution procedure is carried out for an equation of generalized Wannier states. See Refs. [10, 21, 29] for the explicit expression of the equation. Since the residual of the equation ($\delta\phi_i$) is well defined for each wavefunction $\phi_i^{(\text{WS})}$, the accuracy of a calculated wavefunction can be rigorously monitored by the residual norm $|\delta\phi_i|$. The residual norm vanishes, when the calculated wavefunction will be exact ($|\delta\phi_i| \rightarrow 0$). When the wavefunction ϕ_i has a large residual norm $|\delta\phi_i|$, a larger number of atoms ($N_i^{(\text{WS})}$) should be assigned inside the localization region so as to reduce the residual norm $|\delta\phi_i|$. In the present code, the assignment is carried out automatically for each wavefunction at each time step. In the calculation with Fig. 3(a), we classify all wavefunction into three classes with different numbers $N_i^{(\text{WS},\text{min})}$; $N_i^{(\text{WS},\text{min})} = 40, 60$ or 80 . The classification procedure is carried out with the averaged value $\delta\phi_{\text{av}}$ of the residual norm among all wavefunctions $\{|\delta\phi_i|\}$. If the residual norm of a wavefunction ($|\delta\phi_i|$) is almost the same as its averaged value ($|\delta\phi_i| \leq 1.2\delta\phi_{\text{av}}$), the number of $N_i^{(\text{WS},\text{min})}$ is set to be the small

one ($N_i^{(\text{WS},\text{min})} = 40$). If the residual norm of a wavefunction ($|\delta\phi_i|$) is slightly larger than its averaged value ($1.2\delta\phi_{\text{av}} \leq |\delta\phi_i| \leq 1.5\delta\phi_{\text{av}}$), the number of $N_i^{(\text{WS},\text{min})}$ is set to be the middle one ($N_i^{(\text{WS},\text{min})} = 60$). If the residual norm of a wavefunction ($|\delta\phi_i|$) is larger than 150 % of its averaged value ($1.5\delta\phi_{\text{av}} \leq |\delta\phi_i|$), the number of $N_i^{(\text{WS},\text{min})}$ is set to be the large one ($N_i^{(\text{WS},\text{min})} = 80$).

When the three control methods with Wannier states, WS-CC, WS-FC1 and WS-FC2 methods, are compared, in Fig. 3(a), with a reference data by the conventional eigen state method, one finds that the flexible control methods, FC1 and FC2 methods, are significantly better in accuracy than the CC method. This statement is clarified in Fig. 3(b), when the trajectories without that of the CC method show a better agreement.

3.2. Discussions

Although the flexible control methods give, in general, a better accuracy during the MD simulation than the CC method, any of the three methods, WS-CC, WS-FC1 and WS-FC2 methods, is sufficient for discussing physical quantities in the present case; For example, the averaged gradient of Fig. 3 is proportional to the Young modulus in the [001] direction (E_{100}), because the stretching motion is realized within a constant velocity. The Young modulus is estimated, commonly among four calculation methods, to be $E_{100} \approx 100\text{GPa}$, where the estimated value may include an error on the order of 10 %. The estimated value is comparable with the experimental bulk value $E_{100} \approx 130\text{GPa}$ but is deviated, owing to the small system size. Satisfactory results are given also for critical stress for cleavage; $\sigma_c = 2.5 - 3.0\text{GPa}$. Moreover the cleavage propagation velocity (not shown) agrees well among the three Wannier state calculations and the eigen-state calculation. Note that the discussion of these quantities in nanocrystalline silicon is given in Ref. [15].

The WS-FC2 method is required in several simulations and one example is the case of Fig. 2(a) or silicon cleavage with Si(111)- 2×1 cleaved surface; The elementary reconstruction process occurs among several bond sites including surface and subsurface layers, [17] and a larger region is required for describing wavefunctions near the cleaved surface. Since the number of wavefunctions near the cleaved surface accounts for only a small fraction, typically 10 %, of the total number of wavefunctions, the total computational cost of the FC2 method is moderate, when compared with the CC method.

Finally we note that a similar flexible control is also used in Krylov-subspace theory, another theory for large-scale-calculation theory. See Appendix of Ref. [21].

4. Concluding remarks

In this paper, we focus the way of accuracy control in dynamical process or MD simulation. Flexible control methods are proposed so as to realize large-scale process (MD) calculation, in which the electronic freedoms are determined optimally at each

time step.

Since nature (or electronic structure) of physical system can change during a dynamical process, flexible control methods proposed here are crucial, generally, among large-scale calculations, when one would like to achieve a proper balance between accuracy and computational cost.

Acknowledgments

This work is supported by a Grant-in-Aid from the Ministry of Education, Science, Sports and Culture of Japan. Numerical calculation was partly carried out in the Japan Atomic Energy Research Institute, the Institute for Solid State Physics, University of Tokyo, and the Research Center for Computational Science, Okazaki.

- [1] Galli G 2000 Phys. Status Solidi B**217** 231
- [2] Wu S Y and Jayamathi C S 2002 Phys. Rep. **358** 1
- [3] Mauri F Galli G and Car R 1993 Phys. Rev. B**47** 9973
- [4] Li X-P Nunes R W and Vanderbilt D 1993 Phys. Rev. B**47** 10891
- [5] Ordejón P Drabold D A Grumbach M P and Martin R 1993 Phys. Rev. B**48** 14646
- [6] Goedecker S and Colombo L 1994 Phys. Rev. Lett. **73** 122
- [7] Kohn W 1996 Phys. Rev. Lett. **76** 3168
- [8] Hoshi T and Fujiwara T 1997 J. Phys. Soc. Jpn. **66** 3710
- [9] Roche S and Mayou D 1997 Phys. Rev. Lett. **79** 2518
- [10] Hoshi T and Fujiwara T 2000 J. Phys. Soc. Jpn. **69** 3773; cond-mat/9910424
- [11] Ozaki T and Terakura K 2001 Phys. Rev. B**64** 195126
- [12] Tsuruta K Totsuji H and Totsuji C 2001 Phil. Mag. Lett. **81** 357
- [13] Soler J M Artacho E Gale J D García A Junquera J Ordejón P and Sánchez-Portal D 2002 J. Phys.:Condens. Matter **14** 2745
- [14] Bowler D R Miyazaki T and Gillan M J 2002 J. Phys. Condens. Matter **14** 2781
- [15] Hoshi T and Fujiwara T 2003 J. Phys. Soc. Jpn. **72** 2429; cond-mat/0210366
- [16] Takayama R Hoshi T and Fujiwara T 2004 J. Phys. Soc. Jpn. **73** 1519; cond-mat/0401498
- [17] Hoshi T Iguchi Y and Fujiwara T 2005 Phys. Rev. B**72** 075323; cond-mat/0409142
- [18] Skylaris C-K Haynes P D Mostofi A A and Payne MC 2005 J. Chem. Phys. **122** 084119
- [19] Takayama R Hoshi T Sogabe T Zhang S-L and Fujiwara T 2006 Phys. Rev. B**73** 165108; cond-mat/0503394
- [20] Hoshi T Takayama R Iguchi Y and Fujiwara T 2006 Physica B **376-377** 975; cond-mat/0508277
- [21] Hoshi T and Fujiwara T 2006 J. Phys. Condens. Matter **18** 10787; cond-mat/0610563
- [22] Ozaki T 2006 Phys. Rev. B**74** 245101
- [23] Kohn W 1973 Phys. Rev. B**7** 4388
- [24] Kohn W 1993 Chem. Phys. Lett. **208** 167
- [25] Marzari N and Vanderbilt D 1997 Phys. Rev. B**56** 12847
- [26] Hoshi T and Fujiwara T 2001 Surf. Sci. **493** 659
- [27] Andersen O K Saha-Dasgupta T and Ezhov S 2003 Bull. Mater. Sci. **26** 19
- [28] Geshi M Hoshi T and Fujiwara T 2003 J. Phys. Soc. Jpn. **72** 2880
- [29] Hoshi T 2003 Doctor Thesis (Tokyo: School of engineering, University of Tokyo)
- [30] Kwon I Biswas R, Wang C Z, Ho K M and Soukoulis C M 1994 Phys. Rev. B **49** 7242
- [31] Pandey K C 1981 Phys. Rev. Lett. **47** 1913
- [32] F. Ancilotto F Andreoni W Selloni A Car R and Parrinello M 1990 Phys. Rev. Lett. **65**, 3148
- [33] Csányi G Albaret T Payne M C and DeVita A 2004 Phys. Rev. Lett. **93** 175503
- [34] Pérez R and Gumbsch P 2000 Phys. Rev. Lett. **84** 5347
- [35] Stekolnikov AA Furthmüller J and Bechstedt F 2002 Phys. Rev. B **65** 115318